Available online at www.sciencedirect.com
ScienceDirect
Ceramics International 36 (2010) 773–780
CERAMICS INTERNATIONAL
www.elsevier.com/locate/ceramint

Low toxicity binder systems for tape cast $Ce_{0.9}Gd_{0.1}O_{1.95}$ laminates

Trine Klemensø *, Mohan Menon [1], Séverine Ramousse

Fuel Cells and Solid State Chemistry Division, Risø National Laboratory for Sustainable Energy, Technical University of Denmark - DTU, Frederiksborgvej 399, 4000 Roskilde, Denmark

Received 7 September 2009; received in revised form 16 September 2009; accepted 7 October 2009
Available online 13 November 2009

Abstract

Conventional binder systems for tape casting contain toxic phthalate plasticizers and butanone (MEK) as part of the solvent. The effects of exchanging the phthalate with a non-toxic alternative, and butanone with ethanol, were studied on laminates of high-green density CGO ($Ce_{0.9}Gd_{0.1}O_{1.95}$) tapes. Samples were prepared with a binder system containing DBP (dibutyl phthalate) plasticizer and MEK solvent, and with a binder system based on a non-toxic non-phthalate plasticizer and ethanol. In both systems, the weight ratio of plasticizer to the PVB (polyvinyl butyral) binder was varied between 0.4 and 0.7. Substitution to the less toxic binder system had no adverse impacts on the microstructure. In fact, denser packing and improved homogeneity were observed with the non-phthalate-based system at ratio 0.5 indicating improved dispersion in this system. The denser packing also coincided with a maximum in z-shrinkage and molecular weight of the binder system, which could be related to the distribution of the binder system.

Keywords: A. Tape casting; B. Microstructure-final; B. Microstructure-prefiring; B. Porosity; Ga-doped CeO_2

1. Introduction

Ceria doped with e.g. Gd_2O_3 (CGO) or Sm_2O_3 (CSO) shows high oxygen ion conductivity at intermediate temperatures (600–800 °C). The material is therefore considered a promising electrolyte for intermediate temperature solid oxide fuel cells (SOFC) [1–3], and a possibility for SOFC cathode barrier layers [4]. Furthermore, doped ceria can act as a mixed conducting oxide under certain conditions, or be combined with an electronic conductive material, in which case it is of interest for SOFC electrodes [5], flue gas purification [6], and oxygen separation membrane applications [7].

The applications typically imply the doped ceria to be a layer, and part of a multi-layered structure. The ceria may be a thin and dense layer, as e.g. in a SOFC electrolyte, barrier layer, or membrane, or a highly porous layer allowing gas flow, which is necessary in a gas purification device or SOFC electrodes. A production friendly and versatile technique for making the layers is tape casting [4,6,8,9]. The tape casted layers can be joined into multi-layered structures by lamination, where the organic phases of the adjacent layers are merged by thermocompression, and thereby create a bond [8,10,11].

PVB (polyvinyl butyral) binder is commonly the main component of the organic phase in a tape [11–15]. The PVB polymer chains form a network based on hydrogen bonding, which constitutes a matrix for the ceramic particles [13,14]. The utility of PVB is ascribed to benefits like high green strength, good flow properties, solubility in common non-aqueous solvents, compatibility with other organic additives, and a partly stabilizing effect on ceramic dispersions [14]. The PVB chain length determines the specific green mechanical properties. Cho et al. [11] showed that increased molecular weight of the PVB binder resulted in increased green strength and decreased plasticity.

In addition to the PVB, a plasticizer is a key component in the organic binder system. The plasticizer is decisive to avoid stiff and brittle green ceramics, and interacts with the long PVB chains, working either as a ''lubricant'', reducing the frictional forces between the binder polymer chains, or as a ''network breaker'', reducing the attractive forces between the chains [13]. Generally, the plasticizer improves the flexibility at the expense of the strength; and furthermore decreases the elastic modulus, the internal stresses, and the softening temperature of

* Corresponding author. Tel.: +45 4677 5756; fax: +45 4677 5858.
E-mail address: trkl@risoe.dtu.dk (T. Klemensø).
[1] Present address: REC Wafer Norway AS, 3908 Porsgrunn, Norway.

0272-8842/$36.00
doi:10.1016/j.ceramint.2009.10.019

the green component [13–16]. The properties are often enhanced with the amount of plasticizer; for instance Pradhan et al. [17] observed decreased transition temperature with increasing amount of plasticizer. The efficiency of the plasticizer depends on the molecular size and the active groups contained. Plasticizers with lower molecular weight and a small number of active groups are generally more efficient. The smaller size entails higher mobility to access and penetrate a cross-linked polymer network [13,14], though if the plasticizer is too small compared to the PVB, the effect may be lost [16]. The effect of the plasticizer also disappears if the plasticizer contains many active groups that will couple with the PVB and instead strengthen the network [16]. Phthalates are commonly used as plasticizers in non-aqueous ceramic processing [15], and it has been proven that plasticizers with an aromatic unit are more efficient in the PVB-based binder systems than aliphatic linear structures [13].

In recent years, industry has become aware of the hazardous effects of phthalates, and development and implementation of alternatives to phthalates are highly desired. However, substituting the binder system may affect the layer ability to laminate, and have adverse impacts on the microstructure, as the binder system influences on the organization of the ceramic particles as described above, though knowledge on the relationship is limited and qualitative [14,17,18].

Azeotropic solvent mixtures containing butanone, e.g. meket (an azeotropic mixture of butanone/MEK and ethanol), are often used in binder systems and in tape casting slurries due to beneficial properties like polymeric solubility, dielectric constant, and evaporation rate [19]. Replacing the MEK with less hazardous ethanol is desirable and facilitates handling, but may also have consequences on the tape quality and on the microstructural level.

The purpose of the present work was to investigate the possibility of using a less toxic binder system for fabricating CGO tapes and multi-layers, and more generally, to contribute to the fundamental understanding of the binder system and the impact it has on the resulting microstructure. High-green density CGO tapes relevant for SOFC electrolytes and oxygen separation membranes, were manufactured using binder systems with conventional DBP plasticizer and MEK solvent, and binder systems with a non-phthalate plasticizer and ethanol solvent. The binder systems and the microstructures in the different processing steps were characterized, with sample characterization focusing on CGO laminates to facilitate shrinkage and porosity measurements.

2. Experimental procedure

2.1. Starting materials and sample preparation

The slurries were prepared by mixing CGO powder (CGO 90/10 uhsa, specific surface area of 30–35 m^2/g, Rhodia, La Rochelle Cedex, France) with meket as solvent, and PVP (polyvinyl-pyrrolidone with molecular weight 10,000 g/mol) as dispersant in the amount of 10 wt% of the powder. The components were ball milled for 48 h before and after addition

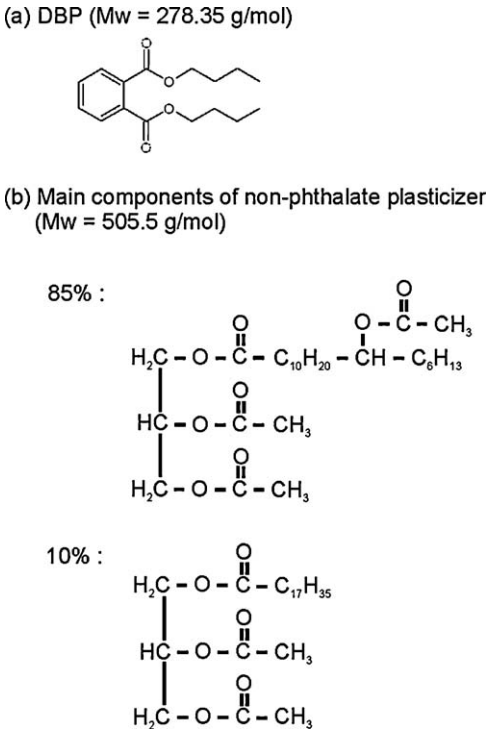

Fig. 1. Main components and average molecular weights of the DBP plasticizer (a) and the non-phthalate plasticizer (b).

of the binder system. The amount of binder system was 36 wt% of the solid CGO and dispersant.

Six different binder systems were prepared based on a typical PVB binder system recipe for tape casting according to [20]. A PVB binder was used, and the plasticizer was either DBP or a non-phthalate alternative based on castor oil. The molecular weights and main components of the two plasticizers are shown in Fig. 1. The binder systems in addition contained minor amounts of release agents, and meket was used as solvent in combination with DBP, and ethanol in combination with the non-phthalate plasticizer. The absolute amounts of the components were kept constant, and only the solvent type, and type and amount of plasticizer was varied. This way, binder systems with plasticizer/PVB ratios of 0.4, 0.5 and 0.7 were prepared.

The slurries were tape cast between doctor blades distanced 500 μm with a casting speed of 20 cm/min. The cast tapes were dried, and laminated at 100 °C into 4-layered samples in a Fuji Lamipacker® Meister6 LPD3212 from Fujipla® (Tokyo, Japan), and subsequently sintered at 1300 °C.

In the following, the binder system and samples prepared with DBP plasticizer will be abbreviated to A, and correspondingly B will denote the system and samples based on non-phthalate plasticizer. The plasticizer/PVB ratio will be included, so that A-0.4 refer to binder system or sample prepared with DBP plasticizer and with the plasticizer/PVB ratio 0.4.

2.2. Measurement techniques

Light scattering particle sizing was used for analysis of particle size distributions of the slurries before tape casting. A

Beckman Coulter LS 13320 instrument with a measurement range of 0.04–2000 μm was applied.

Rheological data were collected on a Haake RheoStress 600 rheometer (Thermo Electron GmbH, Karlsruhe, Germany) equipped with a DC30 temperature control unit using a cone and plate (diameter = 60 mm, $\phi = 1^\circ$, gap = 50 μm). Linear shear rate data were obtained using a preshear of 0.1 s^{-1} for 2 min, followed by 2 min rest. The preshear was included to ensure that the measurements were not influenced by differences in sample history.

The density of the samples was calculated from weight and dimensional measurements, and the porosity estimated from the measured volumes and the theoretical calculated volume of the powder and polymers for the green samples. Open porosity was measured by mercury porosimetry using an Autopore IV 9500 V1.05 from Micromeritics Instrument Corporation (Norcross, GA).

Polished cross-sections of the sintered samples were prepared and the grain boundaries revealed by thermally etching the samples at 1250 °C. The green and sintered microstructures were studied with electron microscopes of the types Zeiss EVO 60 (Oberkochen, Germany) and Hitachi TM-1000 (Pleasanton, CA), and the image analysis software Scion Image [21].

Fourier transform infrared spectroscopy (FTIR) was performed on the surface of green layers using a PerkinElmer Spectrum One FTIR spectrometer (Waltham, MA) in ATR (attenuated total reflection) mode with 4 cm^{-1} resolution. The measurements were done in the range 4000–450 cm^{-1} with 64 scans.

Gel permeation chromatography (GPC) was carried out on the binder solutions with a high-pressure liquid chromatography equipment. The system consisted of a pre-column and a 7.5 mm × 300 mm Asahipak GF-510 HQ column from Shodex (Munich, Germany). The LS-detector (Light scattering detector model TriSEC 270 from Viscotek, Berkshire, UK), UV-detector (UV/vis photodiode array detector model SPD-M10Avp from Shimadzu, Tokyo, Japan), and RI-detector (differential refractometric detector model RID-10A from Shimadzu) were connected in series. The temperature of the columns and the RI-detector was kept at 40 °C, the eluent was 100% methanol with a flow of 0.6 ml/min, and 100 μL of the solutions was injected onto the columns.

3. Results

3.1. Rheology

The liquid binder systems were characterized by steady-state flow measurements. The shear rate sweeps were constrained to maximum shear rates of 10 s^{-1}, which covered the relevant range for the tape casting process. Measurements were carried out after preshear and rest as described in Section 2.2. Fig. 2 shows the linear shear rate sweeps for the binder systems A and B. For comparison, measurements on the binder systems without plasticizers were included and denoted respectively A-0 and B-0. All the binder systems displayed predominant Newtonian behavior with a minor degree of shear thinning. The measurement procedure was seen to result in limited thixotropy.

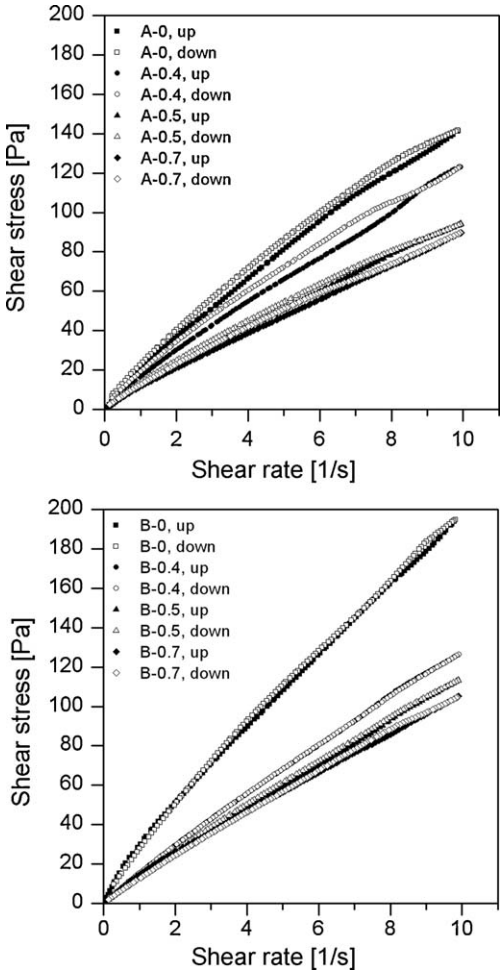

Fig. 2. Linear shear rate sweeps for binder systems A and B.

For both systems, the viscosity decreased with increasing amount of plasticizer. Further, as expected, the viscosity was also observed to decrease with the presence of release agents (not shown here). From the slopes of the graphs, higher viscosity is generally seen for binder systems B compared to the corresponding A. The difference between B-0 and A-0 must be related to the different solvents and their interaction with the PVB binder.

3.2. GPC (gel permeation chromatography)

The size of the polymeric molecules or agglomerates in the binder systems was estimated by GPC. Two runs were performed on all samples, and the same pattern was seen for both runs in all cases. The average from the two runs were calculated and taken as the average molecular weight (Mw) of the binder solution. Fig. 3 illustrates the Mw as a function of the plasticizer/PVB weight ratio. The Mw of binder system B is higher than the corresponding A at all ratios, and with a maximum at ratio 0.5, where the Mw is 74,500 g/mol (B-0.5) versus only 70,700 g/mol for A-0.5 (i.e. 3800 g/mol lower).

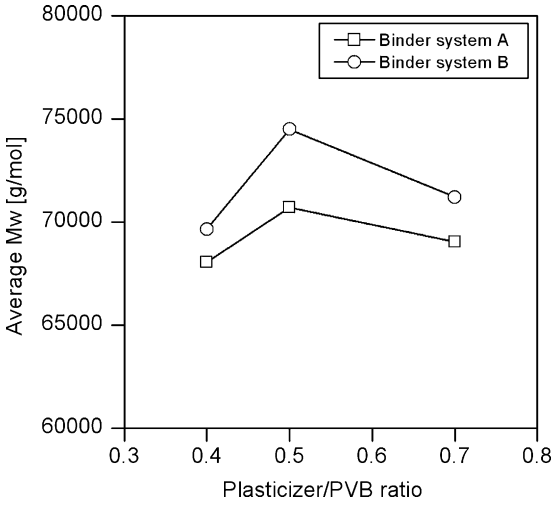

Fig. 3. Average molecular weight (Mw) of the binder systems based on GPC measurements as a function of the plasticizer/PVB weight ratio.

3.3. Porosity, density and shrinkage

The measured porosity and density of the green, de-binded and sintered samples are summarized in Table 1. The porosity was evaluated from weight and dimensional measurements compared to theoretical solid contents (P_{geom}), from mercury porosimetry measurements (P_{Hg}), and microscopy and image analysis (P_{mic}). The geometrically based data (P_{geom} and density) were based on up to 21 measured samples of each type. The average values and standard deviations are shown in Table 1. For microscopy and image analysis data, the average porosity and associated standard deviation were based on 10–11 images of size 35 μm × 45 μm.

No significant difference within experimental error was observed between A and B samples in the green or sintered state. The only exception was for P_{mic} in the sintered state, where B-0.5 displayed significantly lower porosity than A-0.5. However, for the de-binded state, slightly lower open porosity (P_{Hg}) was observed for the A samples (cf. Table 1), in combination with a clear difference in the pore size distributions, shown in Fig. 4. The de-binded B samples showed unimodal pore size distribution, whereas bimodal pore distribution was observed for the de-binded A. Sample A-0.5 further differed from the rest of the A samples showing much coarser pores.

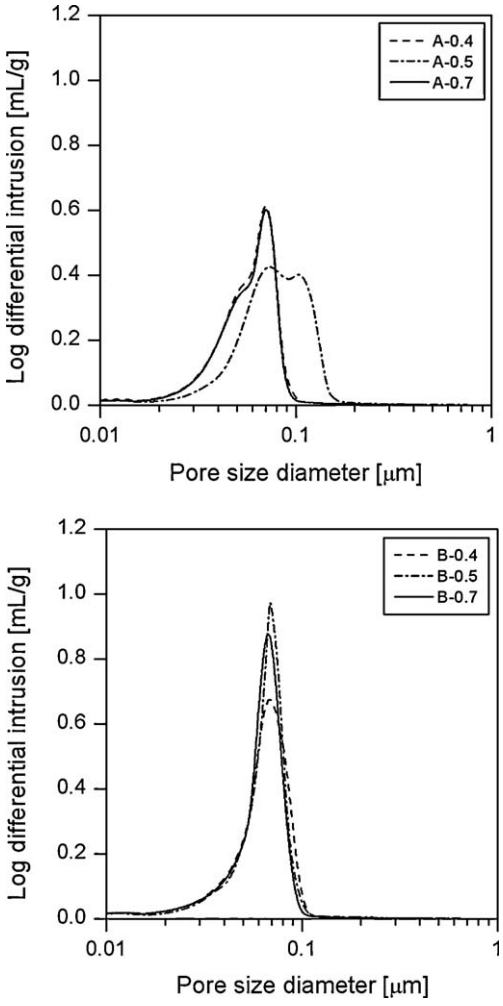

Fig. 4. Mercury porosimetry profiles of de-binded A and B samples.

The sintering shrinkage in-plane (x, y) and thickness (z) are shown in Fig. 5. The data and associated uncertainties were based on up to 21 measured samples of each type. No difference in the in-plane shrinkage between the x- and y-direction was observed, and the average is shown as the lateral shrinkage in Fig. 5. The in-plane shrinkage was similar for A and B samples, however in the z-direction, significantly higher shrinkage was observed for B-0.5 than for the corresponding A-0.5. A maximum in the z-shrinkage occur at ratio 0.5 in both systems, and the z-shrinkage is here in the same range as the in-plane

Table 1
Porosity and density data for green, de-binded and sintered samples based on weight and dimensional measurements (P_{geom}), microscopy and image analysis (P_{mic}), and mercury porosimetry (P_{Hg}).

	Green state		De-binded state	Sintered state			
	P_{geom} [%]	Density [%theory]	P_{Hg} [%]	P_{geom} [%]	P_{mic} [%]	P_{Hg} [%]	Density [%theory]
A-0.4	21 ± 2	78.8 ± 2.2	50	8 ± 3	8 ± 2	–	91.7 ± 2.6
A-0.5	26 ± 3	74.0 ± 3.1	45	10 ± 4	7 ± 1	0	89.7 ± 3.8
A-0.7	19 ± 3	80.6 ± 2.5	48	7 ± 2	6 ± 1	–	93.3 ± 2.3
B-0.4	22 ± 1	78.7 ± 0.6	64	13 ± 3	14 ± 5	–	87.0 ± 3.4
B-0.5	20 ± 7	79.7 ± 7.2	49	5 ± 1	3 ± 1	0	95.0 ± 1.4
B-0.7	21 ± 2	79.5 ± 1.8	51	8 ± 2	6 ± 2	–	92.2 ± 2.3

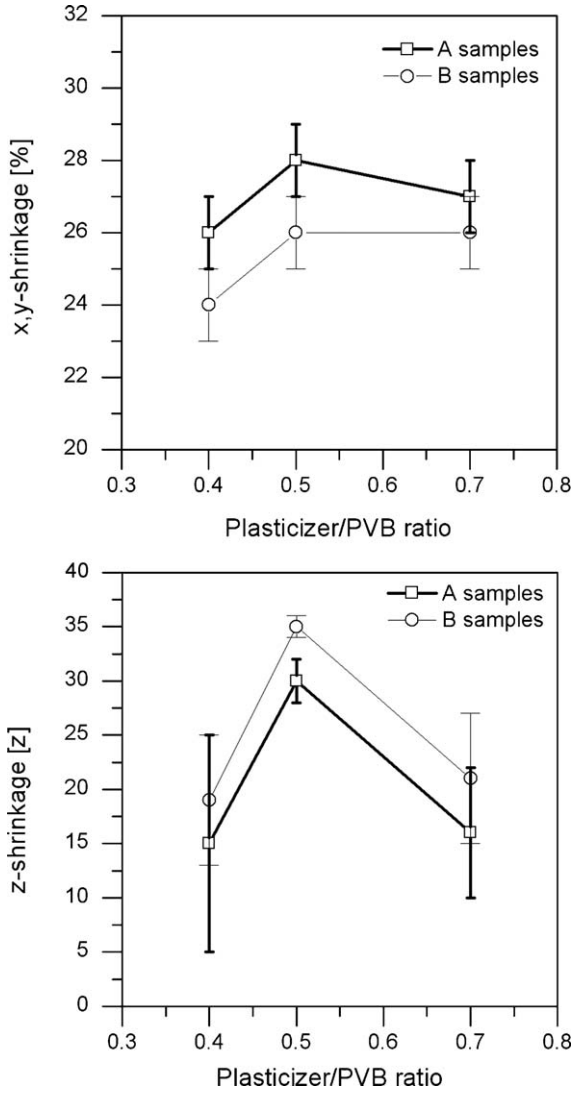

Fig. 5. Lateral (x–y) and thickness (z) sintering shrinkage as a function of the plasticizer/PVB weight ratio.

shrinkage. The higher z-shrinkages at ratio 0.5 was further confirmed by the density measurements in Table 1, showing higher density increases between sintered and green state for A-0.5 and B-0.5.

3.4. FTIR (Fourier transform infrared spectroscopy)

FTIR measurements were done on the green tapes to examine the chemical homogeneity, as segregation of some polymers is known to occur over time [22]. FTIR were done on both surfaces of the cast layers (bottom side and top side), and on up to 8 months old tapes. No relative differences in the spectra between the two surfaces, or between samples of different ages, were observed, indicating that segregation was not an issue in any of the binder systems, and should not affect the laminations.

3.5. Microstructure

A micrograph of the CGO starting powder is shown in Fig. 6. Most of the particles were fine grained (<1 μm) and with

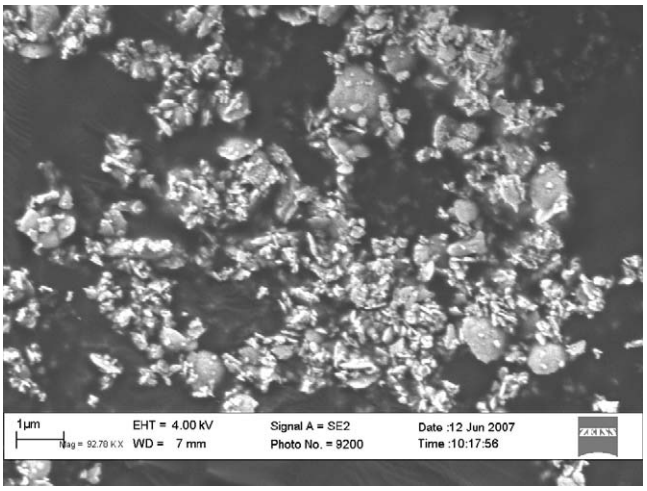

Fig. 6. The starting powder of CGO.

isotropic shape, but a fraction of disc-like bigger CGO particles around 1 μm in size was also observed in the raw powder.

The processed green tapes were examined in cross-section (fractured surface), and on both surfaces of the tape cast layer. None of the sections displayed discernable alignment of the particles, but a difference in the packing was observed between A-0.5 and B-0.5. The surface (bottom) micrographs of these two samples are shown in Fig. 7. The B sample appeared better packed and with fewer agglomerates, and the same pattern was observed in the other sections. The presence of fewer agglomerates in B-0.5 was further confirmed by the PSD (particle size distribution) measurements on the slurries before tape casting, shown in Fig. 8. The 50% quantiles (d_{50}) were respectively 0.46 μm and 0.55 μm for B-0.5 and A-0.5.

Cross-sections of the sintered samples were also examined with microscopy, but qualitative difference was only observed between A-0.5 and B-0.5, with B-0.5 displaying lower porosity, which was also measured by image analyses (cf. Table 1). The heat treated polished samples of A-0.5 and B-0.5 with elucidated grain boundaries are shown in Fig. 9. Again, qualitative difference between A and B samples was only observed at ratio 0.5. The individual grains appeared similar in size, but the agglomerates are more distinct in A-0.5 than in B-0.5.

4. Discussion

4.1. Binder system properties

The plasticizer type and solvent were seen to affect the characteristics of the binder system. Binder system B generally displayed higher viscosity than the corresponding A, and the difference was more pronounced for the higher plasticizer/PVB ratios (cf. Fig. 2). The observed differences in viscosity are likely to reflect the higher molecular weight of the non-phthalate plasticizer compared to DBP, which is almost a factor of 2, and the more branched structure (cf. Fig. 1).

The viscosity decreased with increasing ratio, or plasticizer content, in both binder systems A and B (cf. Fig. 2). As

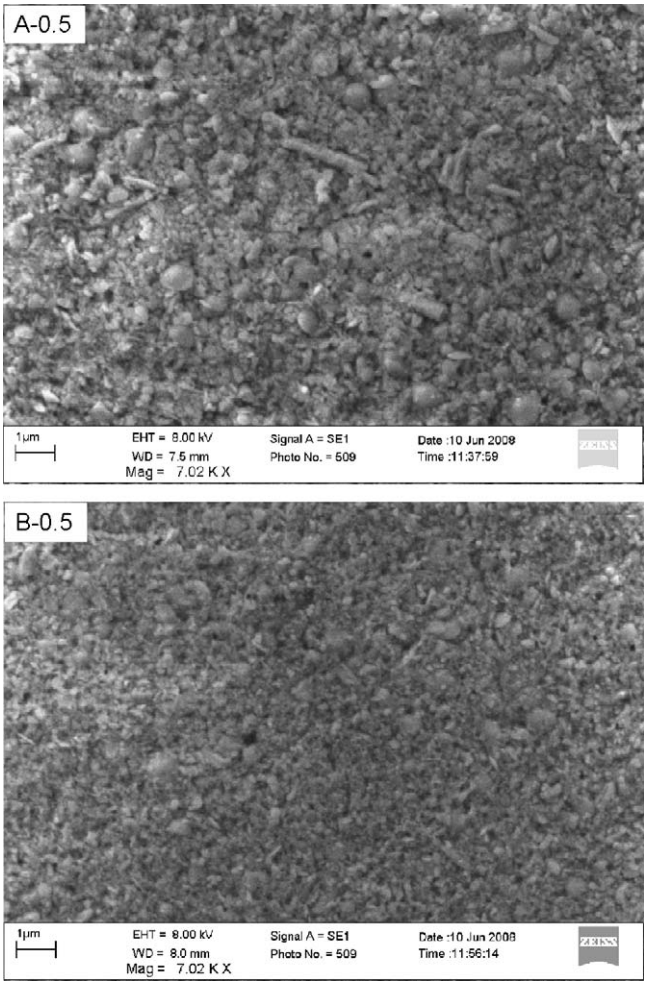

Fig. 7. Micrographs of green tape cast surfaces of A-0.5 and B-0.5.

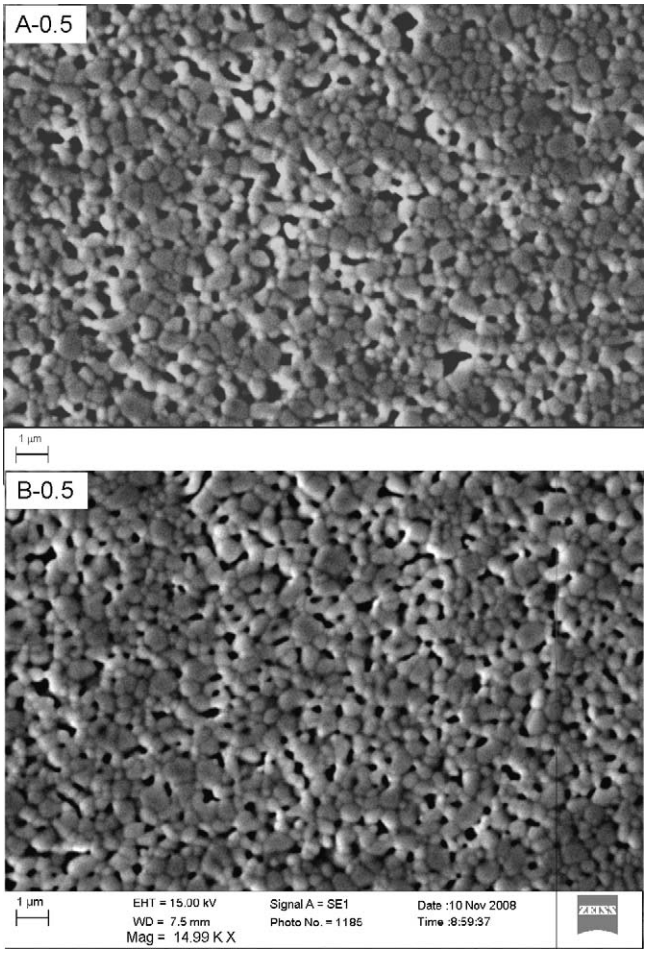

Fig. 9. Micrographs of sintered and thermally etched laminates of A-0.5 and B-0.5.

expected, both plasticizers seemed to work by weakening the intermolecular forces between the PVB chains. A higher efficiency of plasticizer B was indicated by the bigger decrease in slope/viscosity upon addition of the plasticizer (cf. Fig. 2).

The difference in viscosity between A-0 and B-0 must be related to the different solvents. System A contained meket as solvent, and system B ethanol, which can partly explain the difference, since the viscosity of ethanol is a bit higher than for pure MEK, respectively 0.405 mPa s and 1.074 mPa s at 25 °C

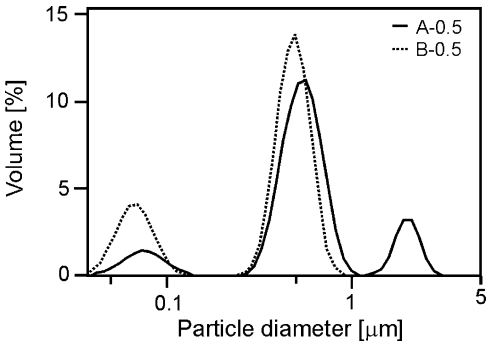

Fig. 8. Particle size distribution of the A-0.5 and B-0.5 slurries before tape casting.

[23]. Based on the visual inspections, the PVB appeared fully dissolved in both solvents. However differences in solubility may affect the dispersion of the PVB polymers, and their mutual interaction degree, which may also play a role [24].

Binder system B also showed higher Mw than the A systems, and a clear maximum in Mw at ratio 0.5 (cf. Fig. 3). The measured molecular weights were taken to reflect the average size of the PVB/plasticizer agglomerates present in the liquid binder system, since the measured Mw values were much higher than the Mw of the separate components. The general higher Mw of system B may be explained by the bigger size and more branched nature of the plasticizer. The observed maximum for especially B-0.5 on the other hand, was unexpected. As explained in Section 1, a plasticizer decreases the intermolecular forces between polymer chains, which inherently will increase the PVB mobility and the average distance between polymers [24]. Based on this, the Mw of the polymer agglomerates would be expected to decrease with the concentration of plasticizer. Instead an increase in Mw was seen from ratio 0.4 to 0.5, and this occurred simultaneously with the viscosity decreasing as expected (cf. Fig. 2). A possible explanation could be the presence of larger, but more loosely bound agglomerates. These could for instance be formed if

some of the plasticizers acted as link between PVB agglomerates, and the combined agglomerate was detected as an assembly. The phenomena would be associated with a specific plasticizer/PVB ratio; at lower ratios fewer plasticizers would act as link, and as the plasticizer concentration increases, the agglomerates will decrease in size.

In both systems A and B, no signs of segregation of the binder system to the surfaces of the tape cast layers were observed (cf. Section 3.4). In addition, based on visual inspections, changing to the binder system B did not deteriorate the tape ability to laminate, indicating no detrimental effect on the glass-transition temperature. The transition temperatures of the two systems were attempted measured by DSC (differential scanning calorimetry), but could not be determined due to a broad transition range, and very low heat absorptions, bordering to the detection limit of the DSC.

4.2. Binder system and resulting microstructure

All samples were prepared from slurries with the same binder system content (i.e. 36 wt% of the solids), and only the binder system components and component ratio were varied. Thus, any microstructural differences were related to the binder system characteristics and the interaction with the solids. Substituting the phthalate with a non-toxic alternative plasticizer, and replacing the MEK solvent with ethanol, resulted in no detrimental microstructural changes in the tape cast and laminated CGO films. On the contrary, finer packing, less agglomeration and improved homogeneity was obtained with especially binder system B-0.5 (cf. Figs. 7–9 and Table 1).

The visible microstructural optimum observed with B-0.5 indicated that this binder system provided the best dispersion of the particles. A similar optimum in the A system was not observed within experimental error, indicating no significant change in the dispersion properties with varying DBP plasticizer content.

The better dispersion obtained with B-0.5 was also indicated by the pore size distribution in the de-binded state (cf. Fig. 4). The de-binded microstructure will be a representation of the spatial distribution of the particles in the green state as sintering has not occurred. The B samples displayed unimodal pore distribution, whereas a bimodal distribution was observed for A, with the unimodal pores indicating a more uniform packing, and a more uniformly distributed binder system.

The de-binded porosity was indicated to be influenced in a minor degree by the Mw of the binder system. The binder systems A-0.5 and B-0.5 showed the higher Mw (cf. Fig. 3), and resulted in the lowest de-binded porosity of the samples (cf. Table 1). Also, the de-binded pore size distributions were indicated to be influenced by the Mw, though in a complex way. A-0.5 appeared to have the coarsest and broadest pore size distribution, whereas B-0.5 appeared to display the sharpest peak. The observed differences in the de-binded state could also be related to the de-binding process, and the formation of different decompositions products. However, the two plasticizers were reported to have similar boiling points, both being below 300 °C, and since the burn-out process was carried out at above 600 °C, this was not believed to be the case.

4.3. Binder system and sintering shrinkage

The in-plane shrinkage was in all cases 24–28%, and no significant variation was observed between the x–y direction, or between different binder systems (cf. Fig. 5). Anisotropic in-plane shrinkage is often seen when tape casting anisotropic powder due to alignment of the long axis of the particles in the casting direction, or in some cases, due to preferred crystallographic alignment [25,26]. The absence of anisotropic in-plane shrinkage for the present tapes is believed due to the CGO powder being mainly isotropic or with disc-shaped geometry (cf. Fig. 6).

Anisotropic z-shrinkage associated with tape casting is also a common phenomena, with the z-shrinkage being often higher than the in-plane. In some cases, the anisotropy has been reported to decrease with increasing solid loadings, and correspondingly lower binder contents, and be a result of the preferential distribution of the polymer phase in the planes normal to z [25]. Thus, anisotropic z-shrinkage is typically related to the de-binding and not the sintering itself. Maximum z-shrinkages were observed in the CGO tapes for both A and B at ratio 0.5, with values of respectively $30 \pm 2\%$ and $35 \pm 1\%$ (cf. Fig. 5), indicating higher binder concentrations in the x–y planes. Higher binder concentrations normal to z could be explained by a degree of alignment of the disc-shaped particles in the x–y plane (cf. Fig. 6), and the reason for the anisotropy being evident only at ratio 0.5 is possibly due to the higher Mw of the binder systems at this ratio (cf. Fig. 3). The significantly higher z-shrinkages at ratio 0.5 did not appear to translate into equally significant increases in the density (cf. Table 1), especially for the A-0.5 case, and the reason for this is not entirely clear based on this work.

5. Conclusion

The structure formation in tape cast and laminated CGO films prepared with different binder systems were investigated. Substituting the plasticizer to a non-toxic alternative, and replacing the MEK in the binder system with ethanol, resulted in no adverse microstructural changes. On the contrary, denser packing and improved homogeneity were observed in one case. The denser packing was believed to reflect improved dispersion properties of the binder system. The denser packing was also seen to coincide with a maximum in z-shrinkage, and a maximum in the molecular weight of the binder system, which could be related to the distribution of the binder system.

Acknowledgements

The authors gratefully acknowledge Lotte Nielsen and Dr. Sokol Ndoni for performing the GPC measurements, Marianne Nielsen for help with the mercury porosimeter, Henrik Paulsen for providing the polished samples, and Dr. Mats Lundberg and Dr. John W. Phair for valuable discussions of the data.

References

[1] L.P. Meier, L. Urech, L.J. Gauckler, Tape casting of nanocrystalline ceria gadolinia powder, J. Eur. Ceram. Soc. 24 (2004) 3753–3758.

[2] J. Cheng, S. Zha, X. Fang, X. Liu, G. Meng, On the green density, sintering behavior and electrical property of tape cast $Ce_{0.9}Gd_{0.1}O_{1.95}$ electrolyte films, Mater. Res. Bull. 37 (2002) 2437–2446.

[3] A. Atkinson, A. Selcuk, Mechanical behaviour of ceramic oxygen ion-conducting membranes, Solid State Ionics 134 (2000) 59–66.

[4] S.P. Simner, M.D. Anderson, M.H. Engelhard, J.W. Stevenson, Degradation mechanisms of La–Sr–Co–Fe–O_3 SOFC cathodes, Electrochem. Solid State Lett. 9 (10) (2006) A478–A481.

[5] B.C.H. Steele, K.M. Hori, S. Uchino, Kinetic parameters influencing the performance of IT-SOFC composite electrodes, Solid State Ionics 135 (1–4) (2000) 445–450.

[6] H. Christensen, Z.S. Rak, A novel diesel particulate converter, Catal. Today 75 (2002) 451–457.

[7] Y. Ji, J.A. Kilner, M.F. Carolan, Electrical conductivity and oxygen transfer in gadolinia-doped ceria (CGO)-$Co_3O_{4-\delta}$ composites, J. Eur. Ceram. Soc. 24 (14) (2004) 3613–3616.

[8] A. Roosen, New lamination technique to join ceramic green tapes for the manufacturing of multilayer devices, J. Eur. Ceram. Soc. 21 (2001) 1993–1996.

[9] M. Chen, H. Zheng, C. Shi, R. Zhou, X. Zheng, Synthesis of nanoparticle Ce–Mg–O mixed oxide as efficient support for methane oxidation, J. Mol. Catal. A: Chem. 237 (2005) 132–136.

[10] J. Gurauskis, A.J. Sánchez-Herencia, C. Baudín, Alumina–zirconia layered ceramics fabricated by stacking water processed green ceramic tapes, J. Eur. Ceram. Soc. 27 (2007) 1389–1394.

[11] Y.-S. Cho, J.-G. Yeo, Y.-G. Jung, S.-C. Choi, J. Kim, U. Paik, Effect of molecular mass of poly(vinyl butyral) and lamination pressure on the pore evolution and microstructure of $BaTiO_3$ laminates, Mater. Sci. Eng. A 362 (2003) 174–180.

[12] C.-W. Cho, J.-H. Hwang, S.-C. Choi, U. Paik, M.-H. Lee, The effect of heat-treatment on the suspension stability and gelation behavior of Li_2O–BaO–Al_2O_3–SiO_2–CaO (LBASC), Mater. Chem. Phys. 99 (2006) 418–423.

[13] D.-H. Kim, K.-Y. Lim, U. Paik, Y.-G. Jung, Effects of chemical structure and molecular weight of plasticizer on physical properties of green tape in $BaTiO_3$/PVB system, J. Eur. Ceram. Soc. 24 (2004) 733–738.

[14] K.Y. Lim, D.H. Kim, U. Paik, S.H. Kim, Effect of molecular weight of poly(ethylene glycol) on the plasticization of green sheets composed of ultrafine $BaTiO_3$ particles and poly(vinyl butyral), Mater. Res. Bull. 38 (2003) 1021–1032.

[15] J.-K. Song, W.-S. Um, H.-S. Lee, M.-S. Kang, K.-W. Chung, J.-H. Park, Effect of polymer molecular weight variations on PZT slip for tape casting, J. Eur. Ceram. Soc. 20 (2000) 685–688.

[16] L.G. Ma, Y. Huang, J.L. Yang, H.R. Le, Y. Sun, Effect of plasticizer on the cracking of ceramic green bodies in gelcasting, J. Mater. Sci. 40 (18) (2005) 4947–4949.

[17] D.K. Pradhan, B.K. Samantaray, R.N.P. Choudhary, A.K. Thakur, Effect of plasticizer on structure–property relationship in composite polymer electrolytes, J. Power Sources 139 (2005) 384–393.

[18] L.A. Ivanchenko, N.D. Pinchuk, A.R. Parkhomei, Effect of the plasticizer on structure formation in purified polydispersed glass ceramic composites, Glass Ceram. 64 (3–4) (2007) 136–139.

[19] Z. Jingxian, J. Dongliang, L. Weisensel, P. Greil, Binary solvent mixture for tape casting of TiO_2 sheets, J. Eur. Ceram. Soc. 24 (1) (2004) 147–155.

[20] G.Y. Onada, Jr., L.L. Hench (Eds.), Ceramic Processing Before Firing, John Wiley & Sons Inc., New York, USA, 1978, pp. 411–448.

[21] Scion Image software, http://www.scioncorp.com/.

[22] V.A. Krauss, A.A.M. Oliveira, A.N. Klein, H.-A. Al-Qureshi, M.C. Fredel, A model for PEG removal from alumina injection moulded parts by solvent debinding, J. Mater. Process. Technol. 182 (2007) 268–273.

[23] D.R. Lide (Ed.), CRC Handbook of Chemistry and Physics, 87th ed., CRC Press, Taylor & Francis Group, LCC, FL, USA, 2006, pp. 6–179.

[24] J. Böhnlein-Mauss, W. Sigmund, G. Wegner, W.H. Meyer, F. Hessel, K. Seitz, A. Roosen, The function of polymers in the tape casting of alumina, Adv. Mater. 4 (2) (1992) 73–81.

[25] J.S. Patwardhan, W.R. Cannon, Factors influencing anisotropic sintering shrinkage in tape-cast alumina: effect of processing variables, J. Am. Ceram. Soc. 89 (10) (2006) 3019–3026.

[26] W.R. Cannon, P.M. Raj, Evolution of sintering anisotropy using 2D finite difference method, J. Am. Ceram. Soc. 92 (7) (2009) 1391–1395.